26) Yang N, Kaur S, Volinia S, *et al.* MicroRNA microarray identifies Let-7i as a novel biomarker and therapeutic target in human epithelial ovarian cancer. Cancer Res 2008;68:10307-14.

27) Galluzzi L, Morselli E, Vitale I, *et al.* miR-181a and miR-630 regulate cisplatin-induced cancer cell death. Cancer Res 2010;70:1793-803.

28) Pogribny IP, Filkowski JN, Tryndyak VP, Golubov A, Shpyleva SI, Kovalchuk O. Alterations of microRNAs and their targets are associated with acquired resistance of MCF-7 breast cancer cells to cisplatin. Int J Cancer 2010.

29) Hong L, Han Y, Zhang H, *et al.* The prognostic and chemotherapeutic value of miR-296 in esophageal squamous cell carcinoma. Ann Surg 2010;251:1056-63.

30) Iorio MV, Visone R, Di Leva G, *et al.* MicroRNA signatures in human ovarian cancer. Cancer Res 2007;67:8699-707.

31) Ladeiro Y, Couchy G, Balabaud C, *et al.* MicroRNA profiling in hepatocellular tumors is associated with clinical features and oncogene/tumor suppressor gene mutations. Hepatology 2008;47:1955-63.

32) Nam EJ, Yoon H, Kim SW, *et al.* MicroRNA expression profiles in serous ovarian carcinoma. Clin Cancer Res 2008;14:2690-5.

33) Xi Y, Formentini A, Chien M, *et al.* Prognostic values of microRNAs in colorectal cancer. Biomark Insights 2006;2:113-121.

34) Dyrskjøt L, Ostenfeld MS, Bramsen JB, *et al.* Genomic profiling of microRNAs in bladder cancer: miR-129 is associated with poor outcome and promotes cell death *in vitro*. Cancer Res 2009;69:4851-60.

35) Nakada C, MatsuurAktsukamoto Y, *et al.* Genome-wide microRNA expression profiling in renal cell carcinoma: significant down-regulation of miR-141 and miR-200c. J Pathol 2008;216:418-27.

36) Tryndyak VP, Beland FA, Pogribny IP. E-cadherin transcriptional down-regulation by epigenetic and microRNA-200 family alterations is related to mesenchymal and drug-resistant phenotypes in human breast cancer cells. Int J Cancer 2010;126:2575-83.

37) Taylor DD, Gercel-Taylor C. MicroRNA signatures of tumor-derived exosomes as diagnostic biomarkers of ovarian cancer. Gynecol Oncol 2008;110:13-21.

38) Thompson JE, Thompson CB. Putting the rap on Akt. J Clin Oncol 2004;22:4217-26.

39) Liu LZ, Zhou XD, Qian G, Shi X, Fang J, Jiang BH. AKT1 amplification regulates cisplatin resistance in human lung cancer cells through the mammalian target of rapamycin/p70S6K1 pathway. Cancer Res 2007;67:6325-32

40) Yoshioka A, Miyata H, Doki Y, *et al.* The activation of Akt during preoperative chemotherapy for esophageal cancer correlates with poor prognosis. Oncol Rep 2008;19:1099-107.

41) Iorio MV, Casalini P, Piovan C, *et al.* microRNA-205 regulates HER3 in human breast cancer. Cancer Res 2009;69:2195-200.

42) Giovannetti E, Funel N, Peters GJ, *et al.* MicroRNA-21 in pancreatic cancer: correlation with clinical outcome and pharmacologic aspects underlying its role in the modulation of gemcitabine activity. Cancer Res 2010;70:4528-38.

43) Switzer CH, Ridnour LA, Cheng RY *et al.* Dithiolethione compounds inhibit Akt signaling in human breast and lung cancer cells by increasing PP2A activity. Oncogene 2009;28:3837-46.

44) Lu J, Kovach JS, Johnson F *et al.* Inhibition of serine/threonine phosphatase PP2A enhances cancer chemotherapy by blocking DNA damage induced defense mechanisms. Proc Natl Acad Sci U S A 2009;106:11697-702.

45) Kim KY, Baek A, Hwang JE *et al.* Adiponectin-activated AMPK stimulates dephosphorylation of AKT through protein phosphatase 2A activation. Cancer Res 2009;69:4018-26.

46) Wang SS, Esplin ED, Li JL *et al.* Alterations of the PPP2R1B gene in human lung and colon cancer. Science 1998;282:284-7.

47) Campbell IG, Manolitsas T. Absence of PPP2R1B gene alterations in primary ovarian cancers. Oncogene 1999;18:6367-9.

48) Wong QW, Ching AK, Chan AW *et al.* MiR-222 overexpression confers cell migratory advantages in hepatocellular carcinoma through enhancing AKT signaling. Clin Cancer Res 2010;16:867-75.

Figure Legends

595 **Table 1.** Relationship between miRNA expression and response to preoperative chemotherapy in patients with esophageal cancer.

Table 2. Correlation between miR-200c expression and clinicopathological features of patient who received preoperative chemotherapy followed by surgery.

600

Figure 1. Kaplan-Meier curves of overall survival rates of 98 patients with esophageal cancer who received preoperative chemotherapy followed by surgery, according to miRNA expression scored as low expression level (below the median value) and high expression (above the median value). High expression levels of miR-200c and miR-21
605 and low expression level of miR-145 correlated significantly with shorter overall survival.

Figure 2. (a, b) Comparison of miR-200c expression in paired tumor and non-tumor tissues of patients with esophageal cancers. The MiR-200c expression level was
610 determined by quantitative reverse transcription-PCR. (a) miR-200c expression in paired tumor and non-tumor samples of 15 patients. (b) Mean expression levels of 15 samples. Data are mean±SD. (c, d) Expression level of miR-200c in cell lines determined by quantitative reverse transcription-PCR. (c) The miR-200c expression level varied in different esophageal carcinoma cell lines. (d) Comparison of miR-200c
615 expression level between cisplatin-resistant cells and parental cells. The expression

level of miR-200c in the established cisplatin-resistant cells (TE8R) is significantly higher than in the parent cells (TE8P). Data are mean±SD. All assays were performed in triplicate, and values represent the mean of three independent experiments.

Figure 3. Effect of inhibition of miR-200c expression on cellular behavior in esophageal carcinoma cell line (TE13). (a) Cells were transfected and 24, 48, 72 and 96 h later their viability was determined by the MTT assay. The viability of control cells, cells transfected with anti-miR-200c, negative control (sc) and mock transfected cells was similar. Inhibition of miR-200c expression had no impact on the proliferative activity. (b) Resistance to cisplatin was determined by the MTT assay 24 h after transfection of cells. Anti-miR-200c-transfected cells are significantly more sensitive to cisplatin than negative control cells. *P<0.01. (c) TE13 cells were stained with PI and Annexin-V 12 and 24 h after treatment with anti-miR-200c or scramble. Early and late apoptotic cells are shown in the right quadrant. (d) Annexin-V-positive cells were quantified by flow cytometry. Data are mean±SD of three independent experiments.

Figure 4. Western blot analysis of SCC cells (TE13). Western blots analysis of differential expression of proteins considered candidate targets of miR-200c at 48 and 72 hours after treatment with anti-miR-200c or scramble. The expression level of each protein was normalized to that of β-actin in each sample. Full-length blots are presented in Supplementary Figure 5. (a) Knockdown of miR-200c expression had no apparent effect on the expression of Apaf-1, TFAP2, and LATS2. (b) Knockdown of

miR-200c expression resulted in decreased expression of phospho-Akt (p-Akt) and increased expression of PPP2R1B at 48h after treatment. But knockdown of miR-200c had no apparent effect on the expression of PPP2CA, SOCS6 and A20.

Author Manuscript Published OnlineFirst on January 19, 2011; DOI:10.1158/1078-0432.CCR-10-2532
Author manuscripts have been peer reviewed and accepted for publication but have not yet been edited.

SUPPLEMENTARY MATERIAL

Supplementary Table 1. Relationship between miRNA expressions and response to preoperative chemotherapy in patients with esophageal cancer

Supplementary Figure 1. Comparison of Ct values of 100 miRNA assays from paired FFPE and Snap-frozen samples. (a) Ct value of RNU48 in RNA isolated from FFPE samples and snap-frozen samples. Data are the mean±SD of three independent experiments. (b) correlation between Ct values of several miRNAs in RNA isolated from FFPE samples and Snap-Frozen samples. R, coefficient of correlation.

Supplementary Figure 2. Kaplan-Meier curves of overall survival rates of 98 patients with esophageal cancer who received preoperative chemotherapy followed by surgery, according to miRNA expression scored as low expression level (below the median value) and high expression (above the median value).

Supplementary Figure 3. Comparison of IC_{50} value for cisplatin-resistant cells (TE8R) and parent cells (TE8P), determined by the MTT assay.

Supplementary Figure 4. Confirmation of anti-miR transfection efficiency. Transfection of anti-miR-200c resulted in suppression of MiR-200c expression at 24h after. Data are mean±SD of three independent experiments.

665 **Supplementary Figure 5.** Results of western blotting (Full-length)

	High expression (n=49)	Low expression (n=49)	P value
miR-200c			
Clinical response CR/PR/NC/PD	0/17/31/1	1/31/16/1	0.009
Pathological response 2/1b/1a/0	1/5/29/14	8/14/16/11	0.007
miR-145			
Clinical response CR/PR/NC/PD	1/21/25/2	0/27/22/0	0.290
Pathological response 2/1b/1a/0	6/9/24/10	3/10/21/15	0.287
miR-21			
Clinical response CR/PR/NC/PD	0/23/24/2	1/25/22/0	0.393
Pathological response 2/1b/1a/0	4/6/27/12	5/13/17/13	0.371

Author Manuscript Published OnlineFirst on January 19, 2011; DOI:10.1158/1078-0432.CCR-10-2532
Author manuscripts have been peer reviewed and accepted for publication but have not yet been edited.

Figure.1 Association of microRNA expression with overall survivals of patients treated with preoperative chemotherapy followed by surgery

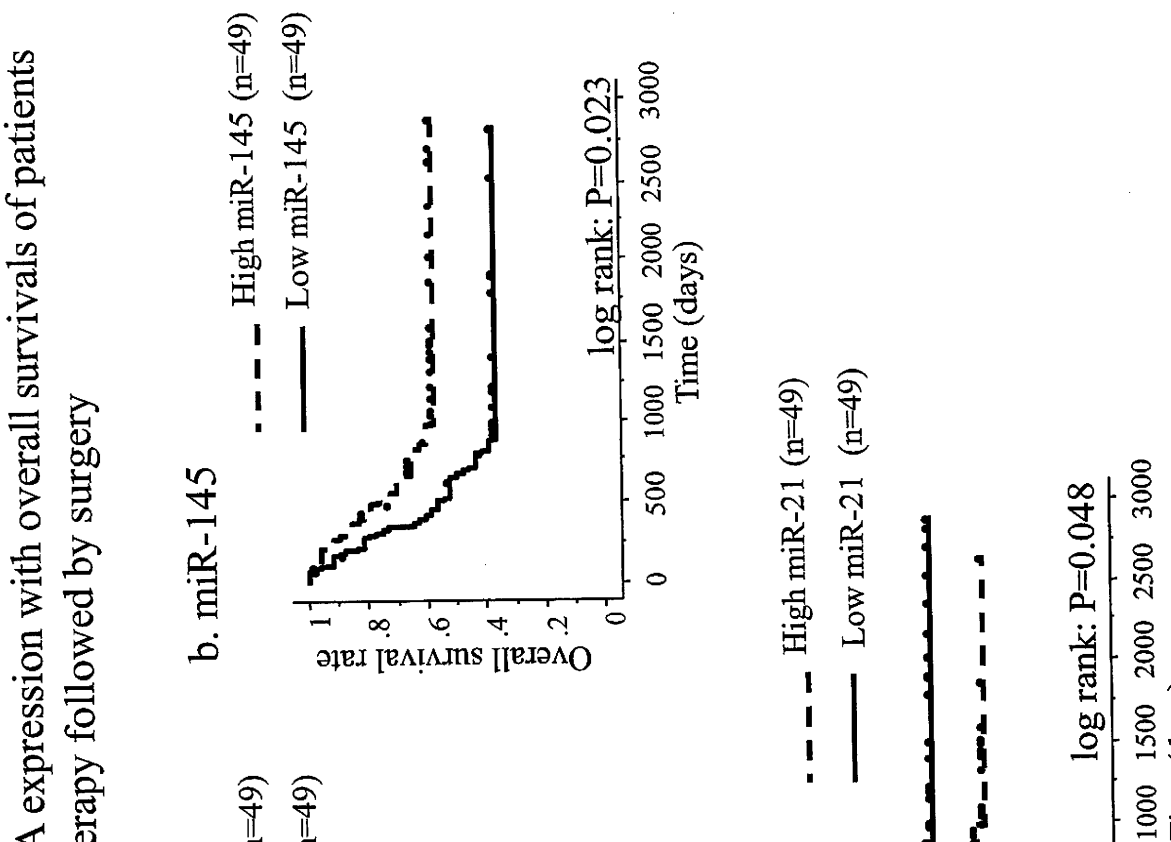

	High expression (n=49)	Low expression (n=49)	P value
Age (mean±SD) (years)	63.2±8.5	60.0±8.6	0.07
Sex			0.774
male	41	43	
female	8	6	
Differentiation			0.278
well-differentiated SCC	10	8	
moderately-differentiated SCC	23	24	
poorly-differentiated SCC	14	10	
other	2	7	
Stage (I/II/III/IV)	1/13/16/19	5/15/12/17	0.262
pT (T1/T2/T3/T4)	2/3/34/10	11/12/20/6	<0.001
pN (N0/N1)	11/38	18/31	0.184
Number of metastatic lymph nodes (mean±SD)	7.59±18.32	4.08±10.23	0.245
pM (M0/M1)	30/19	32/17	0.712
ly			0.022
ly0	46	37	
ly1-3	3	12	
v			0.002
v0	17	33	
v1-3	32	16	
Recurrence			0.276
present	30	26	
absent	19	23	

Figure.2 (a, b) Comparison of miR-200c expression between tumor tissue and non-tumor tissue in each patient (c, d) miR-200c expression in cell lines

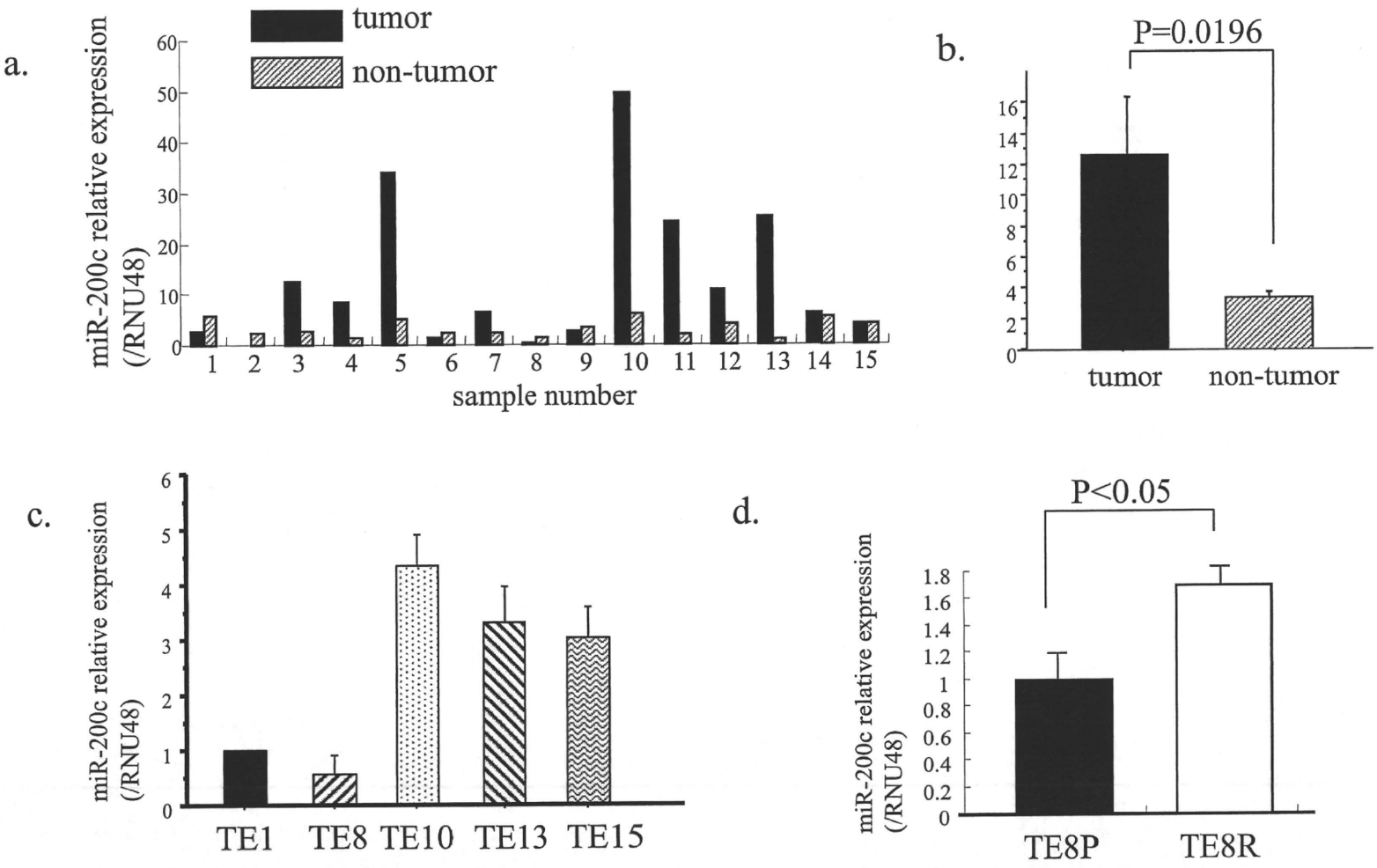

Figure.3 Effect of inhibition of miR-200c expression on cellular behavior in esophageal carcinoma cell line

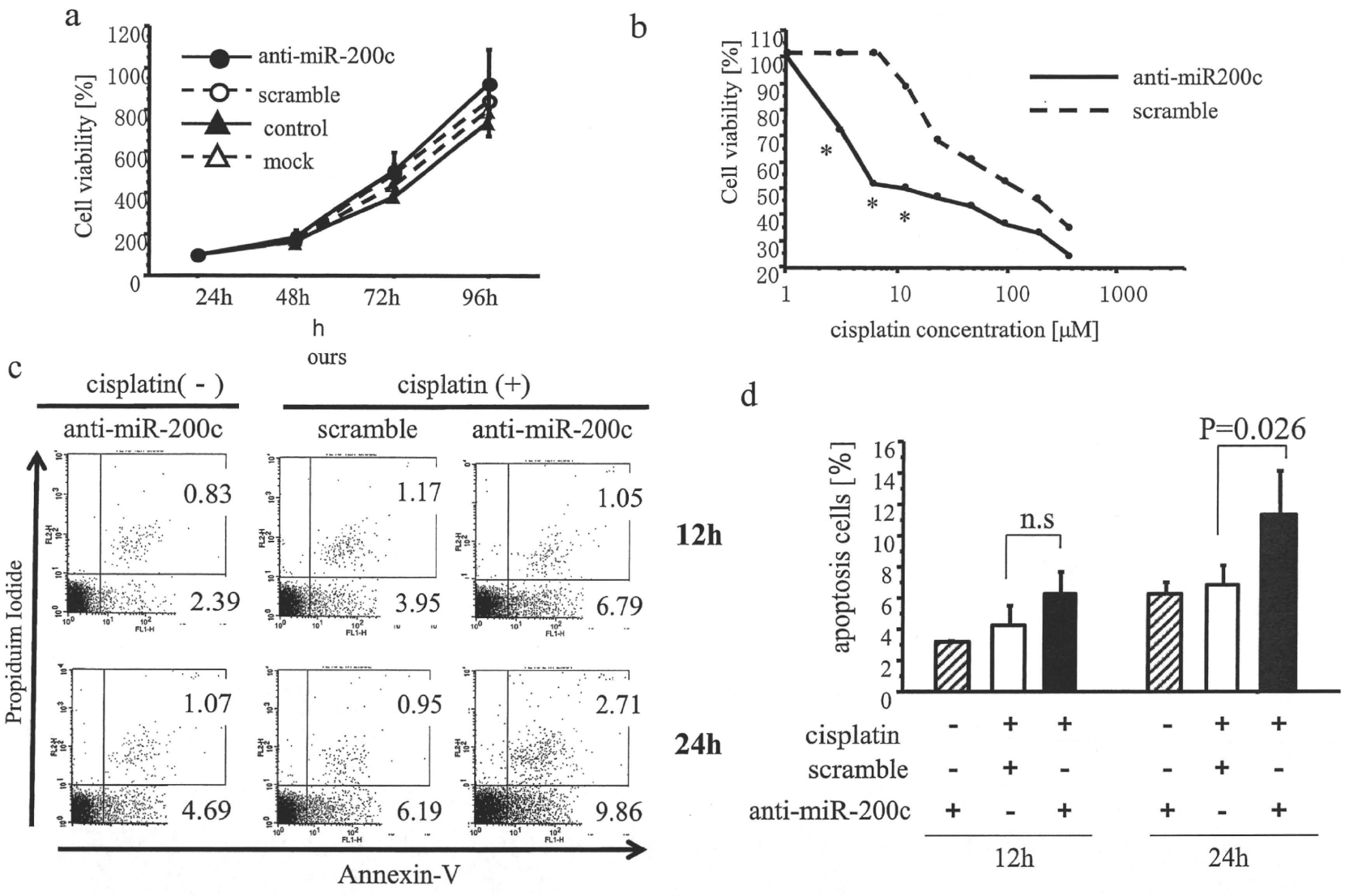

Figure.4 Western blot analysis in SCC cells

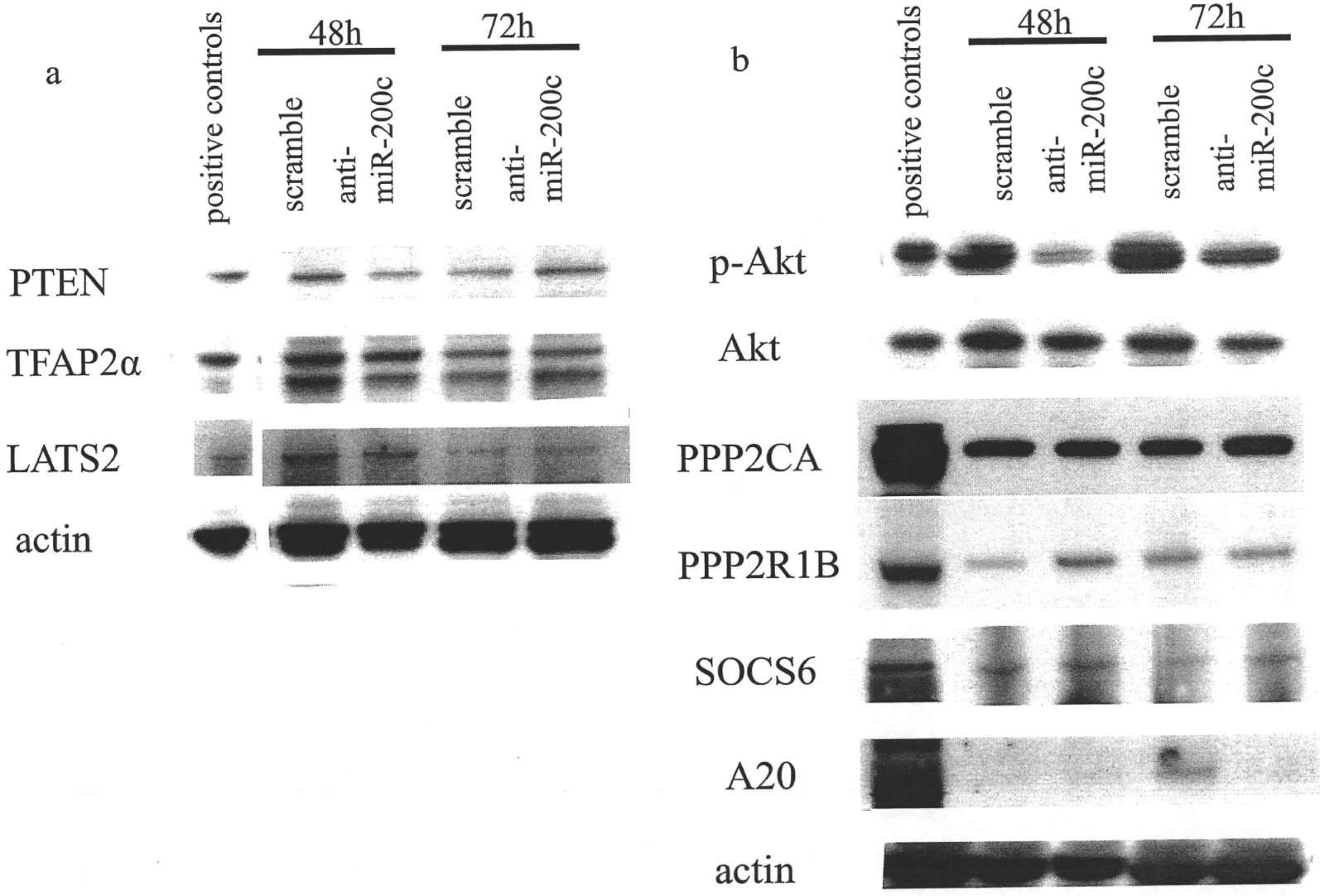

Published OnlineFirst September 7, 2010; DOI:10.1158/1078-0432.CCR-10-0407

Clinical Cancer Research

Jumonji Domain Containing 1A Is a Novel Prognostic Marker for Colorectal Cancer: *In vivo* Identification from Hypoxic Tumor Cells

Mamoru Uemura, Hirofumi Yamamoto, Ichiro Takemasa, et al.

Clin Cancer Res 2010;16:4636-4646. Published OnlineFirst September 7, 2010.

Published OnlineFirst September 7, 2010; DOI:10.1158/1078-0432.CCR-10-0407

Imaging, Diagnosis, Prognosis

Clinical Cancer Research

Jumonji Domain Containing 1A Is a Novel Prognostic Marker for Colorectal Cancer: *In vivo* Identification from Hypoxic Tumor Cells

Mamoru Uemura[1], Hirofumi Yamamoto[1], Ichiro Takemasa[1], Koshi Mimori[3], Hideyuki Hemmi[1], Tsunekazu Mizushima[1], Masataka Ikeda[1], Mitsugu Sekimoto[1], Nariaki Matsuura[2], Yuichiro Doki[1], and Masaki Mori[1]

Abstract

Purpose: This study aimed to identify novel hypoxia-inducible and prognostic markers *in vivo* from hypoxic tumor cells.

Experimental Design: Using carbonic anhydrase 9 and CD34 as a guide for hypoxic tumor cells, laser capture microdissection was used to isolate colorectal cancer (CRC) liver metastases. The samples were analyzed by microarray analysis, in parallel with five CRC cell lines cultured under hypoxic conditions. To evaluate the prognostic impact of the expression of certain genes, samples from a total of 356 CRC patients were analyzed by microarray or quantitative reverse transcription-PCR. *In vitro* mechanistic studies and *in vivo* therapeutic experiments were also done about a histone H3 Lys^9 demethylase, Jumonji domain containing 1A (JMJD1A).

Results: Several candidate genes were identified by microarray analysis of liver metastases and culturing of CRC cells under hypoxic conditions. Among them, we found that JMJD1A was a novel independent prognostic factor for CRC ($P = 0.013$). *In vitro* assays revealed that loss of JMJD1A by small interfering RNA treatment was associated with a reduction of proliferative activity and decrease in invasion of CRC cell lines. Furthermore, treatment with an adenovirus system for antisense JMJD1A construct displayed prominent therapeutic effects when injected into established tumor xenografts of the CRC cell lines HCT116 and DLD1.

Conclusions: JMJD1A is a useful biomarker for hypoxic tumor cells and a prognostic marker that could be a promising therapeutic target against CRC. *Clin Cancer Res; 16(18); 4636–46. ©2010 AACR.*

Hypoxia is a characteristic of many solid tumors. Intratumoral hypoxia affects every major aspect of cancer biology, including cell invasion, metastasis, and determination of cell death (1). Intratumoral hypoxia and/or expression of the hypoxia-related endogenous proteins, vascular endothelial growth factor (VEGF), carbonic anhydrase 9 (CA9), hypoxia-inducible factor-1 (HIF-1), and glucose transporter 1 (GLUT1), are predictive of a poor prognosis in breast cancer (2), head and neck tumors (3), non–small cell lung cancer (4), cervical cancer (5), and colorectal cancer (CRC; ref. 6). There is also evidence that a hypoxia-related gene expression profile is associated with poor prognosis in human cancers (7). Taken together, these findings indicate that hypoxic conditions contribute to aggressive tumor behavior and to a more malignant phenotype.

Many molecules in the hypoxia-response pathway are good candidates for therapeutic targeting (8–10). The anti-VEGF antibody bevacizumab is used clinically for treatment of several human cancers (11), supporting that hypoxia-induced genes are clinically relevant therapeutic targets. Therefore, the identification of novel hypoxia-inducible genes holds great potential for the development of additional cancer therapies.

We aimed to identify, using microarray analysis, a novel prognostic factor and potential therapeutic target *in vivo* using hypoxic tumor cells from hepatic metastases of CRC. We found that Jumonji domain containing 1A (JMJD1A), a histone H3 Lys^9 demethylase, was a useful biomarker for hypoxic tumor cells and a poor prognosis of CRC. JMJD1A functions as a modulator of transcriptional activation of downstream target genes (12–14).

Authors' Affiliations: [1]Department of Surgery, Gastroenterological Surgery, Graduate School of Medicine and [2]Department of Pathology, School of Allied Health Science, Faculty of Medicine, Osaka University, Osaka, Japan; and [3]Department of Surgery and Molecular Oncology, Medical Institute of Bioregulation, Kyushu University, Beppu, Japan

Note: Supplementary data for this article are available at Clinical Cancer Research Online (http://clincancerres.aacrjournals.org/).

M. Uemura and H. Yamamoto contributed equally to this work.

Corresponding Author: Hirofumi Yamamoto, Department of Surgery, Gastroenterological Surgery, Graduate School of Medicine, Osaka University, 2-2 Yamada-oka, Suita City, Osaka, 565-0871, Japan. Phone: 81-6-6879-3251; Fax: 81-6-6879-3259; E-mail: hyamamoto@gesurg.med.osaka-u.ac.jp.

doi: 10.1158/1078-0432.CCR-10-0407

Published OnlineFirst September 7, 2010; DOI:10.1158/1078-0432.CCR-10-0407

Translational Relevance

Hypoxia is a characteristic feature of many solid tumors. Intratumoral hypoxia affects every major aspect of cancer biology. However, it is not easy to detect truly important hypoxia-inducible genes that are related to clinical cancer biology *in vitro* because cancer cells usually exist in chronically hypoxic conditions *in vivo* with complex interactions with several pathways. In this study, we showed that liver metastasis of colorectal cancer is a useful *in vivo* material to identify novel hypoxia-inducible and prognostic markers. This finding has great potential for extending our knowledge of hypoxia-related cancer biology and may provide guidance for developing novel cancer therapies. Furthermore, we have shown that a histone H3 Lys^9 demethylase, Jumonji domain containing 1A (JMJD1A), is a useful prognostic marker that can be a therapeutic target in colorectal cancer using the therapeutic xenograft model.

Because hypoxic tumor cells are likely to be resistant to cancer therapy, the present findings may provide clues for the development of a novel anticancer therapy.

Materials and Methods

Cell culture

HEK293 cells and human colon cancer cell lines HCT116, LoVo, DLD1, and HT29 were obtained from the American Type Culture Collection. The human colon cancer cell line KM12SM was a kind gift from Prof. T. Minamoto (Cancer Research Institute, Kanazawa, Japan). Cells were grown in DMEM supplemented with 10% fetal bovine serum, 100 units/mL penicillin, and 100 μg/mL streptomycin at 37°C in a humidified incubator with 5% CO_2. For culture under hypoxic conditions, cells were grown for up to 72 hours at 37°C in a continuously monitored atmosphere with a 1% O_2, 5% CO_2, and 94% N_2 gas mixture using a multigas incubator (model 9200, Wakenyaku Co.). Cells were cultured in normoxic conditions (21% O_2) as a control/reference.

Clinical samples

Hepatic metastases from CRC patients (n = 15) were consecutively collected exclusively during partial liver resection at Osaka University Hospital between 2000 and 2005. The samples of liver metastasis were embedded in OCT compound and frozen in liquid nitrogen within 10 to 15 minutes of resection. The samples were stored at −80°C until RNA extraction. For microarray analysis, we prospectively collected 214 primary CRC samples from consecutive patients who had curative operations in 2003 to 2006 from Osaka University Hospital and its nine associated hospitals. For quantitative reverse transcription-PCR (qRT-PCR), tumor samples were consecutively collected from a total of 142 CRC patients who had curative surgery from 1998 to 2002 at the Department of Surgery, Medical Institute of Bioregulation, Kyusyu University, and at its three associated institutes. The mean follow-up times were 44.0 ± 14.4 and 43.7 ± 33.5 months, respectively. The clinicopathologic features of patients from each institute, including gender, tumor location, extent of wall invasion, lymph node metastasis, histologic grade, clinical stage, and invasion to vein or lymphatic duct, are shown in Supplementary Table S1A and B.

In this study, none of the patients had preoperative chemotherapy or irradiation. After surgery, patients with stage III/IV tumors were basically treated with 5-fluorouracil–based chemotherapy. The surgical specimens were preserved in paraffin block and used for immunostaining of CD34 and JMJD1A. A piece of each primary CRC tissue sample was collected from the fresh specimens within 30 minutes after resection and stored in RNA Stabilization Reagent (RNAlater, Ambion, Inc.) at −80°C until RNA extraction. The RNA samples were kept at −80°C. For long-time storage, cDNA was routinely synthesized from RNA samples within 4 to 6 weeks after the operation and stored at −20°C. The Human Ethics Review Committee of Osaka University and Kyusyu University approved the use of the resected samples. REMARK criteria for tumor marker studies was used for the preparation of this article (15).

Immunohistochemistry and vessel count

Immunohistochemical analysis was done as described previously (16). Frozen sections (8 μm) were fixed in 4% paraformaldehyde for 5 minutes. The anti-CD34 mouse monoclonal antibody (1:500; Novocastra), anti-human CA9 goat polyclonal antibody (1:200; Santa Cruz Biotechnology), and anti-JMJD1A rabbit polyclonal antibody (1:100; Proteintech Group, Inc.) were incubated on the slides for 1 hour at room temperature. For negative controls, nonimmunized immunoglobulin G (Vector Laboratories) was used as a substitute for the primary antibody. Double staining of CD34 and CA9 was carried out as described previously (17). CA9 expression was scored as follows: 0, no staining; 1, weak staining; 2, moderate staining; and 3, strong staining. $CD34^+$ blood vessels were counted under a microscope at ×100 magnification. Ten visual fields were selected randomly in each portion of the metastatic CRC lesion, and the mean vessel counts per visual field were calculated. Vessel count was scored as follows: 0, no vessel staining; 1, 1 to 3 vessels; 2, 4 to 10 vessels; and 3, >10 vessels.

Western blot analysis

Western blot analysis was done as described previously (18). The membrane was incubated with the primary antibodies at the appropriate concentrations (1:800 for JMJD1A and 1:1,000 for actin) for 1 hour.

Published OnlineFirst September 7, 2010; DOI:10.1158/1078-0432.CCR-10-0407

Laser capture microdissection and microarray analysis

Laser capture microdissection (LCM) was done using the LM200 LCM system (Arcturus Engineering) as described previously (17). The quality check of total RNA and microarray analysis were carried out as described previously (19) using an oligonucleotide microarray covering 30,000 human probes (AceGene; DNA Chip Research, Inc. and Hitachi Software Engineering Co. Ltd.).

qRT-PCR

After reverse transcription, real-time monitoring of PCRs was done using the LightCycler system (Roche Applied Science) for quantification of mRNA expression (18). A housekeeping gene, porphobilinogen deaminase (PBGD), was used as an internal control (20). The PCR primers used in this study are listed in Supplementary Table S2.

Transfection of small interfering RNA

For small interfering RNA (siRNA) inhibition, double-stranded RNA duplexes targeting human *JMJD1A* (5′-AGAAGAAUUCAAGAGAUUCCGGAGG-3′/5′-CCUCCG-GAAUCUCUUGAAUUCUUCU-3′) and negative control siRNA were purchased in a Stealth RNAi kit (Invitrogen). CRC cell lines were transfected with siRNA using Lipofectamine RNAiMAX (Invitrogen) according to the manufacturer's protocols.

Invasion assay

The invasion assay was done using Transwell cell culture chambers (BD Biosciences) as described previously (21). Briefly, 5×10^5 cells were seeded in triplicate on the Matrigel-coated membrane. After 48 hours, cells that had invaded the undersurface of the membrane were fixed with 100% methanol and stained with 1% toluidine blue. Four microscopic fields were randomly selected for cell counting.

Generation of an adenoviral antisense construct to JMJD1A

The entire coding sequence of human JMJD1A was amplified by RT-PCR with primers 5′-GGTACCGCCAC-CATGGTGCTCACGCTCGGAG-3′ and 5′-CTCGAGT-TAAGGTTTGCCAAAACTGGATTCAC-3′ using mRNA prepared from KM12 cells. Adenoviral vectors containing

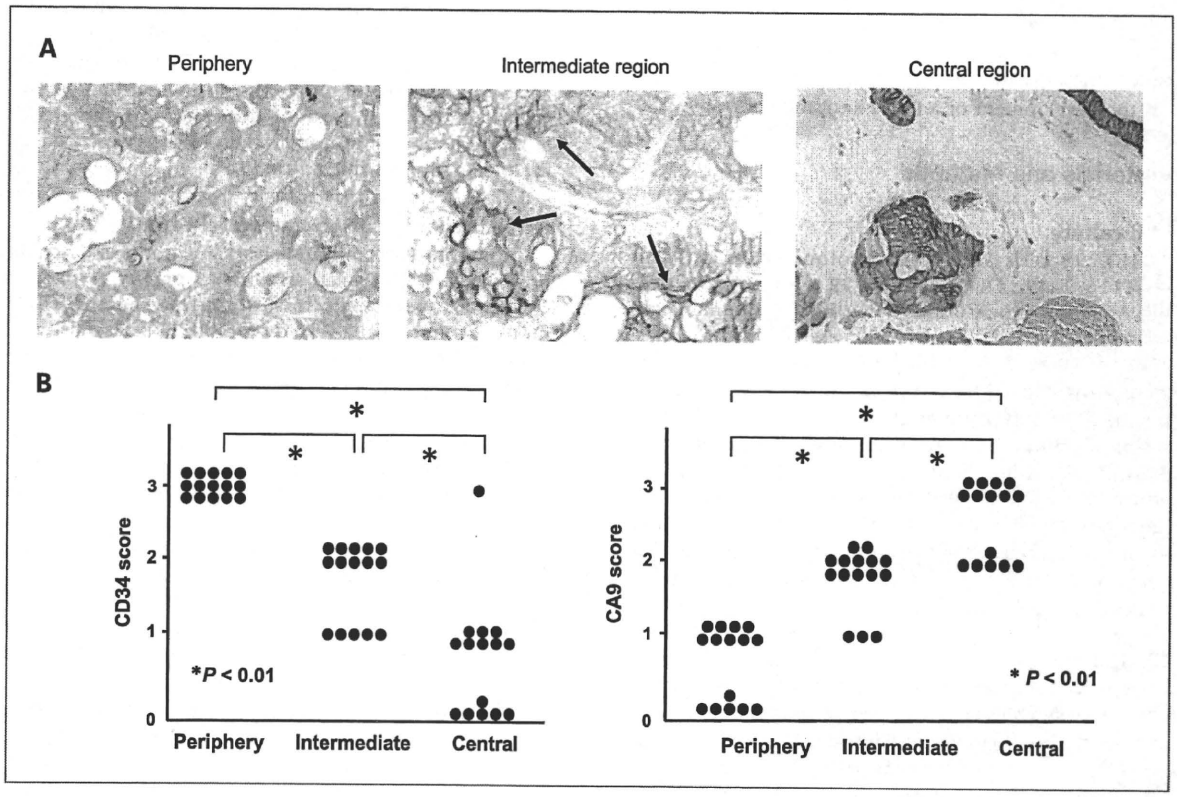

Fig. 1. Immunohistochemistry of CD34 and CA9 in liver metastasis. A, liver metastasis was double stained for CD34 as a vascular endothelial cell marker and CA9 as a hypoxic tumor cell marker. Tumor vessels (CD34; pink) decreased from the periphery to the central region. Conversely, CA9 expression in tumor cells (brown) increased from the periphery to the central region. Black arrows indicate that the intensity of CA9 staining was enhanced 80 μm from the tumor vessel. Magnification, ×400. B, scoring CD34 and CA9 staining. The CD34 score decreased significantly from the periphery to the central region ($P < 0.01$); conversely, the CA9 score increased significantly ($P < 0.01$). The details of each score are described in Materials and Methods. We then did LCM of $CD34^-CA9^+$ tumor cells around the central region and $CD34^+CA9^-$ tumor cells around the periphery of CRC liver metastasis.

Published OnlineFirst September 7, 2010; DOI:10.1158/1078-0432.CCR-10-0407

antisense JMJD1A were constructed using the AdEasy Adenoviral Vector System (Stratagene; ref. 21). Adenoviral recombination and preparation of infectious particles in HEK293 cells were described previously (22).

Treatment of established tumor xenografts by intratumoral injection of an adenoviral antisense construct to JMJD1A

Subcutaneous xenografts of the CRC cells DLD1 and HCT116 were established in nude mice ($n = 5$) by injection of 5×10^6 cells. After 1 week, when the tumor size reached 100 to 200 mm^3, Ad-Mock, adenoviral antisense (Ad-AS) construct to JMJD1A (1.0×10^9 plaque-forming units per injection), and NaCl solution were injected into tumors on days 7, 9, 11, and 13.

Statistical analysis

Statistical analysis was done using the StatView 5.0 program (Abacus Concepts, Inc.). The Kaplan-Meier method was used to examine disease-free survival, and the log-rank test was used to determine statistical significance. A Cox proportional hazard model was used to assess the risk ratio with simultaneous contributions from several covariates. Statistical analysis was done using the Student's t test or Fisher's exact test for categorical data and the Mann-Whitney U test for nonparametric data. Correlation significance was assessed using Pearson's correlation coefficient test. Values of $P < 0.05$ denoted a statistically significant difference.

Results

Immunohistochemistry of CD34 and CA9 in liver metastasis

To identify *in vivo* hypoxic tumor cells, we first did double staining of CD34 and CA9 using 15 hepatic metastases of CRC (Fig. 1A). The $CD34^+$ vascular endothelial cells (stained pink) significantly decreased from the periphery to the intermediate region to the central region of the metastasis. In contrast, CA9 expression in the tumor cells (stained brown) increased from the periphery to the central region (Fig. 1B). It was noteworthy that the intensity of CA9 staining became strong 80 μm from a tumor vessel in the intermediate region (Fig. 1A, middle), suggesting that CA9 is a sensitive marker for hypoxic tumor cells in hepatic metastasis of CRC.

LCM and microarray analysis

Using CA9 and CD34 as markers, $CD34^+CA9^-$ tumor cells in the periphery (Fig. 1A, left) and $CD34^-CA9^+$ tumor cells in the central region (Fig. 1A, right) were collected by LCM. After confirmation that high-quality RNA was derived from the tumor cells, 12 paired samples were subjected to microarray analysis.

The mean value of the fold induction in the central region relative to the periphery was calculated. Thirty genes with the greatest fold inductions are shown in Table 1, with the fold induction level ranging from 3.00 to 1.65. These 30 genes included well-known hypoxia-inducible genes, namely, egg-laying–defective nine homologue 3 (EGLN3), VEGF, endothelin-1 (EDN1), adrenomedullin (ADM), and peroxisome proliferator-activated receptor γ (PPARG). In addition, we found only a few reports that were related to hypoxia for prolyl-4-hydroxylase 1 (P4HA1), trefoil factor 3 (TFF3), endoplasmic reticulum oxidoreductin1-like (ERO1L), fatty acid binding protein (FABP1), and JMJD1A.

To investigate whether there were other novel hypoxia-inducible gene candidates, five colon cancer cell lines were subjected to microarray analysis after exposure to either hypoxic or normoxic conditions for 72 hours. We found that RNA levels were upregulated under hypoxic conditions in the genes that ranked 7th, 10th, 11th, 13th, 14th, 22nd, 23rd, 24th, and 29th in Table 1. The maximum induction of these genes was above 2.5-fold, which is comparable with the fold induction of known hypoxia-inducible genes (range, 1.2- to 8.3-fold).

Selection of novel biomarkers for malignant primary CRC

The well-known hypoxia-inducible genes VEGF, EDN1, EGLN3, TFF3, ADM, FABP1, and PPARG, listed in Table 1, were reported as poor prognostic factors for human malignancies (12, 23–32). To identify other genes that could serve as novel prognostic factors, we prospectively analyzed 214 CRC tissue samples using the same microarray chip; clinical data on disease recurrence were known for these samples. Our analysis indicated that JMJD1A (rank 9) and ADM (rank 21) were both significant prognostic markers for CRC. Although ADM was reported as a prognostic factor for ovarian cancer (30), JMJD1A has not been reported as a biomarker for human malignancies. Therefore, we subsequently focused on JMJD1A. A significant linear correlation of JMJD1A mRNA levels between microarray and qRT-PCR was observed ($P = 0.0004$; Supplementary Fig. S1A). Disease-free survival curves also showed that a high level of JMJD1A mRNA was a significant predictor of a shorter disease recurrence rate ($P = 0.0054$; Supplementary Fig. S1B). Supplementary Table S3 summarizes univariate and multivariate analyses for disease-free recurrence in the 214 CRC patients.

JMJD1A expression determined by qRT-PCR and immunohistochemistry

qRT-PCR analysis indicated that induced JMJD1A expression was 2.52-fold higher in the central region of liver metastasis compared with the periphery ($P = 0.0094$; Fig. 2A). Immunohistochemistry revealed that JMJD1A expression in the tumor cells (stained brown) increased from the periphery to the central region (Fig. 2B). Notably, the intensity of JMJD1A staining became strong 80 μm from a tumor vessel; this was also the case with CA9 staining. An approximately 3- to 6-fold induction of JMJD1A RNA was measured by qRT-PCR in the majority of CRC cell lines examined (Fig. 2C).

Published OnlineFirst September 7, 2010; DOI:10.1158/1078-0432.CCR-10-0407

Table 1. Microarray analysis of metastatic lesions in liver

Microarray data of liver metastasis				Representative gene symbol*	Gene ID	Accession
Rank	Mean fold	SD	Mann-Whitney *P*			
1	3	5.430236	0.41892	REG3A	5068	M84337
2	2.9	2.369342	0.02295	Unknown genes		BQ959777
3	2.68	1.069202	0.0003	EGLN3	112399	DQ975379
4	2.06	2.49874	0.45292	OLFM4	10562	NM_006418
5	2.04	1.009858	0.00042	VEGF	7422	AL136131
6	1.96	1.268504	0.00745	P4HA1	5033	NM_000917
7	1.91	1.447802	0.00324	RPGR	6103	NM_001034853
8	1.9	0.608637	0.01792	TFF3	7033	NM_003226
9	1.87	0.820366	0.00221	JMJD1A	55818	NM_018433
10	1.86	1.412287	0.15513	ACVR1	90	NM_001111067
11	1.84	1.227838	0.19141	RHOU	58480	NM_021205
12	1.81	1.428676	0.07419	EDN1	1906	NM_001955
13	1.79	1.173002	0.03123	OBSL1	23363	NM_015311
14	1.79	1.222501	0.0675	RGNEF	64283	NM_022448
15	1.78	0.78898	0.04157	HMBOX1	79618	NM_024567
16	1.78	1.274998	0.13091	FLJ21062	79846	NM_001039706
17	1.76	0.666219	0.00022	VEGF	7422	XM_052673
18	1.75	0.797286	0.14891	PSPH	5723	XM_028728
19	1.75	0.816036	0.02277	Unknown genes		AF189585
20	1.74	2.031618	0.62558	REG3A	5068	NM_002580
21	1.74	0.770142	0.00791	ADM	133	NM_001124
22	1.69	0.984528	0.00876	TARDBP	23435	NM_007375
23	1.68	0.965191	0.07556	SLCO1C1	53919	NM_017435
24	1.68	1.798507	0.84936	Unknown genes		AC009141
25	1.66	1.70151	0.18091	Unknown genes		AC005961
26	1.66	1.094456	0.52537	FABP1	2168	NM_001443
27	1.65	0.880628	0.1842	ERO1L	30001	NM_014584
28	1.65	0.885692	0.13719	SULF1	23213	NM_015170
29	1.65	0.618633	0.02434	ATP1B1	481	NM_001677
30	1.65	0.488769	0.00268	PPARG	5468	NM_015869

(*Continued on the following page*)

Survival survey

qRT-PCR was done using 142 independent CRC samples obtained from other institutes. High expression of JMJD1A RNA (n = 71, cutoff: median value; Supplementary Table S1B) was a significant prognostic factor with regard to cancer-related survival (P = 0.0108; Table 2). When analyzed with several clinicopathologic parameters that were statistically significant by univariate analysis, such as lymph node metastasis (P < 0.0001), lymphatic invasion (P < 0.0001), venous invasion (P = 0.0013), and depth of tumor invasion (P = 0.0008; Table 2), multivariate Cox regression analysis revealed that JMJD1A expression remained an independent prognostic factor (P = 0.0139; Table 2). As for the relationship between JMJD1A expression and each clinicopathologic characteristic, no significant difference was noted for age, gender, tumor location, and other factors (Supplementary Table S1B).

Effects of JMJD1A expression on growth and invasion of CRC cells

To assess the potential relevance of JMJD1A as a therapeutic target, *in vitro* knockdown experiments were done. Western blot analysis showed a significant reduction in the JMJD1A protein after siRNA treatment (Fig. 3A). A significant growth inhibition was observed in siRNA-treated HCT116 and DLD1 cell lines (P < 0.05 for each; Fig. 3B). Furthermore, invasion assays indicated that siRNA treatment significantly decreased the number of invaded cells of the two CRC cell lines when compared with control treatments (P < 0.05 for each; Fig. 3C).

Treatment of established tumor xenografts with an adenoviral construct of antisense JMJD1A

Similar to siRNA treatment, Ad-AS JMJD1A significantly decreased *in vitro* cell growth of the two CRC cells at a multiplicity of infection (MOI) of 100 (P < 0.05 for